Bioprocessing and Biomass Technology

Journal homepage: https://bioprocessing.utm.my

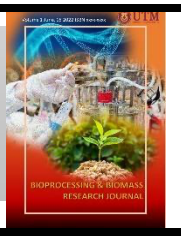

Research Article

Optimization of Carboxymethyl Cellulose from Ozonated Empty Fruit Bunch for Biofilm Fabrication

Danish Akmal[a], Zhahidah Husna Hassan[a], Mohd Asmadi Mohammed Yussuf[a*], Nur Hafizah Ab Hamid[a], Mahadhir Mohamed[a], Amnani Shamjuddin[a]

[a] *Chemical Reaction Engineering Group (CREG), Faculty of Chemical and Energy Engineering, Universiti Teknologi Malaysia, 81310 Skudai, Johor, Malaysia*

ARTICLE INFO

Article History:
Received 11 February 2026
Received in revised form 15 April 2026
Accepted 21 April 2026
Available online 30 June 2026

Keywords:
Ozonated Empty Fruit Bunch
Carboxymethyl Cellulose
Response Surface Methodology
Biofilm Fabrication

ABSTRACT

Carboxymethyl cellulose (CMC) derived from lignocellulosic biomass has gained interest in biodegradable film fabrication. In this study, CMC was synthesized from ozonated empty fruit bunches (EFB). The parameters for synthesizing the CMC were screened and optimized focusing on the degree of substitution (DS) of CMC. The CMC was then used for biofilm fabrication. The parameters for CMC production and its effect on DS were evaluated by using response surface methodology (RSM). All parameters significantly influenced the DS of CMC, and the optimal DS achieved is 0.69 at 15% NaOH, cellulose: sodium monochloroacetate (SMCA) of 1:2, reaction temperature of 55 °C and a reaction time of 1.5 hrs. The characterization of CMC at different DS by thermogravimetric analysis (TGA) and scanning electron microscopy (SEM) shows high resistance to thermal degradation 500 °C with a more irregular surface for DS 0.69 as compared to lower DS. Using the CMC with DS 0.69 for biofilm fabrication, the biofilm achieved tensile strength up to 34.43 MPa, elongation break at 45% with solubility less than 10% both at room and high temperatures the formulation of biofilm consisted of CMC (4.99 wt.%), citric acid (2.49 wt.%), glycerol (1.26 wt.%), and water (91.26 wt.%). Overall, the optimized CMC can be used as a polymer matrix in biofilm fabrication, producing biofilm with high tensile strength, elongation, and low solubility.

INTRODUCTION

Oil palm residue is among various biomass sources that are abundant and underutilized, especially in palm oil countries. Oil palm biomass consists mainly of oil palm fronds (OPF), empty fruit bunches (EFB), mesocarp fibre, palm kernel shell (PKS), and oil palm trunks (OPT), with EFB accounting for approximately 20.4% of total biomass generation annually (Mahmud & Chong, 2021). Biomass contains cellulose, hemicellulose, lignin, and extractives which are normally known as lignocellulosic biomass. Notably, EFB exhibits a relatively high cellulose content (40–45%) (Aisyah et al., 2024), exceeding that of OPF (35–40%) (Zhang et al., 2023), mesocarp fibre (30-35%), and PKS (25–30%) (Kaniapan et al., 2021), making it a suitable feedstock for cellulose-derived products.

Conventional pretreatment methods to isolate cellulose from biomass generally use alkali, acidic or steam-explosion that combines with bleaching, resulting in high chemical consumption. Furthermore, ozonolysis has emerged as an effective alternative that can selectively degrade lignin while preserving the cellulose chain (Rachtanapun et al., 2021). Although ozonolysis operates under mild conditions with lower chemical consumption and mainly avoids degradation of cellulose, ozonolysis treatment could improve cellulose accessibility and uniformity (Ab Rasid et al., 2021).

Once extracted, cellulose can be used to produce several derived products such as microcrystalline cellulose (MCC), cellulose nanocrystals (CNC), and carboxymethyl cellulose (CMC). Carboxymethyl cellulose, a water-soluble cellulose

*Corresponding Author
E-mail address: mohdasmadi@utm.my
DOI address: 10.11113/bioprocessing.v5n1.92
ISBN/©UTM Penerbit Press. All rights reserved
Faculty of Chemical and Energy Engineering, Universiti Teknologi Malaysia

ether has attracted significant attention due to its wide application such as emulsifiers, pharmaceuticals, thickeners, drilling, paper, and biofilms (Song & Othman, 2022).

The applications of CMC are strongly dependent on CMC's degree of substitution (DS). Low DS values (<0.4) result in limited solubility and rigid structures, making CMC more suitable for binders or paper-related applications rather than film formation (Hasanin et al., 2025). In contrast, CMC with a higher DS value (approximately 0.6–0.9) has been widely reported to exhibit favourable film-forming properties, balancing flexibility and mechanical integrity (Zhang et al., 2023). At higher DS values (>1.0), CMC becomes highly hydrophilic and readily soluble in water, which may reduce mechanical stability is valuable for applications such as thickeners, stabilizers, and pharmaceutical or food formulations, which require rapid solubility (Macieja et al., 2022).

The synthesis of CMC involves the activation of cellulose by alkali in an organic solvent and etherification. The process can also have a side reaction that produces a by-product. The alkalization, etherification and side reaction were presented in **Eqn. (1)–(3)**, respectively. Then, the cellulose reacts with NaOH to form alkali cellulose, which increases the reactivity of the hydroxyl group in the cellulose. The alkali cellulose is then subjected to etherification at hydroxyl groups using sodium monochloroacetate (SMCA) to produce CMC. In addition, an additional side reaction may occur between NaOH and SMCA producing sodium glycolate, water and salt (Churam et al., 2024).

$$[C_6H_7O_2(OH)_3]_n + nNaOH \rightarrow [C_6H_7(OH)_2ONa]_n + nH_2O \quad \textbf{Eqn. (1)}$$

$$[C_6H_7O_2(OH)_2ONa]_n + nClCH2COONa \rightarrow [C_6H_7O_2(OH)_2OCH_2COONa]_n + nNaCl \quad \textbf{Eqn. (2)}$$

$$2nNaOH + nClCH_2COOHNa \rightarrow HOCH_2COONa + nH_2O + nNaCl \quad \textbf{Eqn. (3)}$$

The DS of CMC strongly depends on the synthesis parameters (Rachtanapun et al., 2021). For instance, CMC synthesized using different solvent mixtures and NaOH concentrations exhibited a DS range from approximately 0.575 to 0.906 (Nguyen et al., 2022). Similarly, CMC synthesized from empty fruit bunch (EFB) cellulose after ionic liquid pretreatment showed a DS of 0.82 under optimised conditions, highlighting the influence of pretreatment and reagent composition on substitution degree (Nguyen et al., 2022).

In biofilm fabrication, CMC often acts as the polymer matrix with the addition of cross-linking agents such as citric acid and plasticizers such as glycerol (Rahman et al., 2021). Glycerol acts as a plasticizer to improve the flexibility and elongation of the biofilm by reducing intermolecular interactions within the polymer matrix. On the other hand, citric acid acts as a crosslinking agent, enhancing mechanical strength and reducing the solubility of the biofilm via the formation of ester linkages with the polymer. Previous studies have reported that variations in these formulation parameters significantly influence tensile strength, elongation at break, and solubility behaviour (Hidayati et al., 2021; Nazry, 2023). With a varying ratio of biodegradable films produced from seaweed waste, the CMC and glycerol mixture showed tensile strengths ranging from approximately 23-39 MPa, indicating that both plasticizer level and polymer content govern mechanical performance (Hidayati et al., 2021). Another study on CMC bioplastics using deep eutectic solvent (DES) plasticizers content reported tensile strength values from 0.25 to 41 MPa and elongation at break increasing from 4.75 to 19%, with water solubility strongly affected by plasticizer composition (Nazry, 2023). These findings indicate that biofilm performance is highly influenced by the formulation and interaction between polymer matrix composition and plasticizer.

Despite much research on CMC synthesis and biofilm development, the influence of parameters in the synthesis of CMC on DS and mechanical properties and solubility of biofilm has not yet been established. Thus, it is essential to address this limitation as the characteristics of the CMC-based biofilm rely on the DS of CMC. Therefore, this study aims to screen the parameters of CMC and optimize the operating parameters in the synthesis of CMC for DS. The optimized CMC was used in biofilm fabrication to evaluate its mechanical and solubility properties.

MATERIALS AND METHOD

Materials

The empty fruit bunch was obtained from Felda Taib Andak Palm Oil Mill, Kulai, Johor, Malaysia. Initially, EFB was air-dried for 8 hrs to reduce the moisture content. Then, dried EFB was oven-dried at 100 °C in an oven to ensure a complete moisture removal. The dried EFB was further ground and sieved using a mechanical siever shaker. Particles with a size of approximately 0.5 and 0.3 µm were collected and used for subsequent treatments and analyses. Sodium hydroxide (NaOH) pellet, hydrogen peroxide (H_2O_2) 50%, isopropanol alcohol, sodium monocholoacetate (SMCA, $C_2H_2ClNaO_2$), methanol (95%), ethanol (95%), glacial acetic acid, glycerol (99.7%) and citric acid monohydrate were all manufactured by Sigma-Aldrich Co and used as received.

Ozonolysis Pretreatment of EFB

The EFB was ground and sieved to a particle size of 0.3 µm. The sieved EFB was moisturized to 30% moisture content. The sample was then ozonated in the OzBiONY reactor. The concentration of ozone was 60 mg/m^3 with a flow rate of 1.5 L/min supply to the reactor. The ozonolysis process was performed for 1.5 hrs at constant mixing. The ozonated sample was then washed with 70% v/v of acetone-water solution (3:7 v/v ratio) at a solid-to-liquid ratio of 1:10. The mixture was stirred using a mechanical stirrer, ensuring lignin dissolution in acetone. After that, the mixture was filtered to recover the solid fraction. The solid fraction was then rinsed thoroughly with distilled water until the water solution turned clear. The washed sample was then dried in an oven for 15 hrs at 65 ℃ (Husna et al., 2025).

Screening of CMC

CMC was prepared according to Ab Rasid et al (2021). A 15 g of cellulose with a size of 200-500 µm was placed in a beaker and 450 mL of isopropanol was added. Then, it was alkalized with 50 mL of NaOH (10% to 50%) (w/v) concentration under continuous stirring. After that, SMCA with a cellulose to SMCA ratio (1:1 to 1:2) was added to initiate the carboxymethylation reaction. Next, the reaction mixture was sealed and heated in an oven at 65 °C for 3 hrs. After that, the solid product was separated by removing the

liquid phase in the beaker. The solid product was then suspended in 100 mL of ethanol. It was then neutralized to pH 7.0 by using glacial acetic acid (10 mL to 30 mL), depending on the initial pH of the solid product. After neutralization, the neutralized solid was then recovered using a vacuum filter and washed with ethanol and methanol. The washing was carried out by pouring 50 mL of ethanol onto the solid phase, repeated 5 times and followed by a final wash with 50 mL of methanol. The solid product was then oven-dried at 65 °C for 12 hrs before grinding into CMC powder.

For the screening of CMC, the experimental ranges for the screening study were used to generate the design of experiment (DOE) by using a fractional factorial design in Statistica Software, as summarized in **Table 1**. Based on this design, 8 individual experimental runs were produced and labelled as sample A1 to A8 with different parameter conditions. The range of parameters was selected based on the literature (Fouad et al., 2024; Masrullita et al., 2022; Rahman et al., 2021; Thepwat et al., 2025). Approximately, 10% NaOH concentration have been shown to be sufficient amount for activation and alkalization of cellulose, while higher concentrations up to 50% can enhance the cellulose swelling and etherification efficiency (Rahman et al., 2021). The SMCA loading ratio was selected as the highest SMCA loading 1:2, to improve substitution efficiency (Thepwat et al., 2025). In addition, the particle size is also considered a process parameter. The lowest range for particle size is <200 µm to favour higher surface area and accessibility of the reactive site (Fouad et al., 2024). Larger particle sizes up to 500 µm are normally used for CMC synthesis (Masrullita et al., 2022).

Table 1 Standards used for proximate analysis

Parameters	Symbol	Range and Levels	
		-1 (low)	+1 (high)
NaOH conc. (%)	X_1	10	50
SMCA loading ratio	X_2	1:1	1:2
Particle size (µm)	X_3	<200	<500

Optimization of CMC

The CMC synthesis method was performed according to literature (Ab Rasid et al., 2021). As demonstrated in **Table 2**, the ranges of the experimental parameters for CMC optimization were NaOH concentration (10 to 20%), cellulose to SMCA ratio (1:1 to 1:1.2), reaction temperature (35 to 55 ℃) and reaction time (1 to 2 hrs). These parameter ranges were used in central composite design (CCD) in Statistica Software. The CCD was selected due to its ability to model quadratic responses using a minimal number of experiments and incorporating centre points for accurate estimation of optimization.

Based on this design, 10 experimental runs were produced and labelled as sample B1 to B10. Samples B1 to B8 represent different parameter combinations, while B9 and B10 has same parameter combination as replicates to assess experimental error and reproducibility of results.

Biofilm Fabrication

CMC-based biofilms were prepared using the solvent casting method with varying formulations of CMC, glycerol, citric acid, and distilled water. Initially, 80 mL of the distilled water was heated, and CMC was gradually added under continuous stirring to ensure complete dissolution. 20 mL of distilled water was heated separately at 65 °C followed by the addition of glycerol (0.1, 0.55 and 1.0 mL) and citric acid (1.0, 1.75 and 2.5 mL). Both solutions were maintained at 65 °C for 5 min before the glycerol–citric acid solution was added to the CMC solution and mixed thoroughly. The mixture was then homogenized for 15 min and subjected to ultrasonic treatment using an ultrasonic water bath for 5 minutes at room temperature (25 ℃) to remove entrapped air bubbles. Approximately 40 mL of the degassed solution was cast into silicone moulds and dried in an oven at 60 °C for 48 hrs. The dried biofilms were then removed from the moulds and conditioned at ambient conditions before further characterization. Mixed design using Statistica Software was employed, and the ranges of each parameter are shown in **Table 3**.

Table 2 Experimental ranges and coded levels of process variables for CMC optimization

Factor	Symbol	-1 (low)	0 (Centre)	+1 (High)
NaOH conc. (%)	X_1	10	15	20
SMCA loading ratio	X_2	1.0	1.1	1.2
Temp. (°C)	X_3	35	45	55
Time (hr)	X_4	1.0	1.5	2.0

Table 3 The boundaries of the mixture design for DOE for biofilm

Factor	Symbol	-1	+1
Glycerol	X_1	0.2%	2%
Citric Acid	X_2	2%	5%
CMC	X_3	3%	10%

RESULTS AND DISCUSSION

Screening of CMC

The screening of CMC parameters was performed to evaluate the influence of parameters on the physicochemical properties of CMC, with a focus on the DS. The experimental results are summarized in **Table 4**, which shows that the DS values ranged from 0.1 to 0.6 depending on the parameters producing CMC. These values fall within the range reported in previous studies, where DS values typically vary from approximately 0.1 to above 1.0 depending on the cellulose source and reaction conditions (Rahman et al., 2021). The DS variations were primarily influenced by changes in cellulose: SMCA loading ratio, NaOH concentration, and particle size, indicating that the extent of etherification depends on these parameters. Generally, a higher SMCA loading ratio contributed to increased DS, reflecting improved availability of etherifying agents. However, this increase in DS was not linear, suggesting that excessive reagent concentration does not necessarily enhance substitution efficiency. Similar trends were observed for yield, viscosity, and purity, indicating that structural modification of cellulose occurred alongside changes in chemical composition. The predictive model for the screening characterizations was generated by the Statistica Software and is presented in **Eqn. (1) – (6)**:

$$Y_1 = 352-5.5X_1+42.8X_2-0.2X_3+3.5X_1X_2-3.5X_2X_3 \quad \textbf{Eqn. (1)}$$

$$Y_2 = 3.15-0.002X_1-0.75X_2-0.004X_3-0.0035X_1X_2+0.0035X_2X_3 \quad \textbf{Eqn. (2)}$$

$$Y_3 = 1.63-0.002X_1-0.33X_2-0.001X_3-0.008X_1X_2+0.001X_2X_3 \quad \textbf{Eqn. (3)}$$

$$Y_4 = 37.9-0.23X_1-18.03X_2+0.39X_2X_3 \quad \textbf{Eqn. (4)}$$

$$Y_5 = 14.4+0.77X_1+32.5X_2+0.01X_3-0.65X_1X_2+0.04X_2X_3 \quad \textbf{Eqn. (5)}$$

$$Y_6 = 0.35+0.3X_1-0.17X_2-0.004X_3-0.015X_1X_2+0.002X_2X_3 \quad \textbf{Eqn. (6)}$$

The arrangement between observed and predicted values is presented in **Figure 1**, which presents the parity plots for the selected response variables. A strong correlation between predicted and experimental values was observed with coefficients of determination (R^2) exceeding 0.95, except for purity (R^2 = 0.87), confirming the reliability of the screening model. Minor deviations between predicted and experimental data may be attributed to the changes in fibre structure due to the ozonolysis treatment. which affects the accessibility of cellulose hydroxyl groups for the etherification reaction.

The interaction effects between parameters are further illustrated in the 3D plots shown in **Figure 2**. As shown in **Figure 2 (a)**, the DS values of 0.6 and higher were primarily observed at cellulose: SMCA loading ratios between 1.6 and 2.2 and NaOH concentrations ranging from 28% to 52%, indicating that effective etherification requires sufficient alkalization and adequate availability of the etherifying agent (Wahyuni et al., 2019). For the interaction between particle size and NaOH concentration in **Figure 2 (b)**, high DS values were generally obtained across particle sizes of 200-500 µm. However, at smaller particle sizes (approximately 200 µm), the optimal region was restricted to NaOH concentrations between 28% and 36%. This suggested that although smaller particles provide greater surface area, they to excessive NaOH concentrations (Yuliasmi et al., 2019). In **Figure 2 (c)**, high DS values were achieved when the cellulose: SMCA loading ratio exceeded 1.4, indicating that the Cellulose: SMCA loading ratio plays a more dominant role than particle size in substitution efficiency.

Based on the 3D surface plot, under the condition of SCMA loadings between the range of 1.6 to 2.2, combined with NaOH concentrations ranging from 28% to 52%, DS exceeding 0.6 can be achieved. The combined effect of alkalization and etherifying agent availability played a crucial role in enhancing the substitution reaction, leading to improved carboxymethylation efficiency. Outside this optimal region, a clear reduction in DS was observed, suggesting that insufficient alkalinity or overly harsh chemical conditions can hinder the substitution process. These results emphasized the importance of carefully regulating both cellulose: SMCA loading ratio and NaOH concentration to achieve a desired DS value.

Optimization of CMC

Reaction temperature and reaction time were included as parameters for optimization of CMC as shown in **Table 5**. The DS increases with increasing NaOH content, cellulose: SMCA loading, and reaction temperature suggesting improved cellulose activation and etherification efficiency.

Table 4 Data from the screening of parameters for CMC synthesis

Sample	Cellulose: SMCA	NaOH Conc (% w/v)	Particle Size (µm)	Yield (%) Y_1	Viscosity (cP) Y_2	Density (g/cm³) Y_3	Moisture Content (%) Y_4	Purity (%) Y_5	Degree of Substitution Y_6
A1	1:1	30.00	<200	224.30	1.90	1.41	22.52	49.50	0.30
A2	1:1	50.00	<200	181.40	1.80	1.67	23.06	47.00	0.60
A3	1:2	30.00	<200	327.30	1.60	1.59	16.50	48.00	0.20
A4	1:2	50.00	<200	337.00	1.40	1.83	25.74	45.70	0.10
A5	1:1	30.00	>500	202.90	1.40	1.28	18.50	36.40	0.10
A6	1:1	50.00	>500	125.80	1.20	1.33	16.46	49.50	0.20
A7	1:2	30.00	>500	336.80	1.80	1.55	14.20	36.10	0.50
A8	1:2	50.00	>500	347.00	1.60	1.93	19.22	23.10	0.50

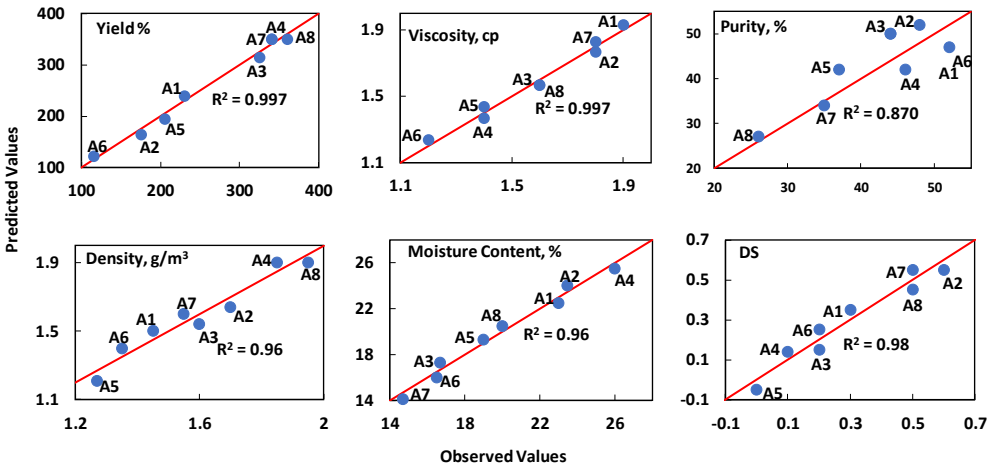

Figure 1 The parity plots of CMC at different parameters for screening

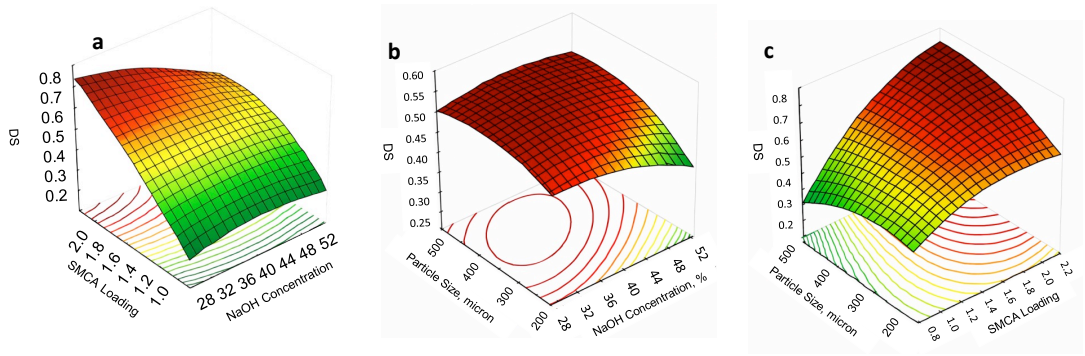

Figure 2 3D response surface plots showing the interactive effects of process variables on the degree of substitution (DS) of carboxymethyl cellulose (CMC) within the range of 0.6–0.8: **(a)** SMCA loading and NaOH concentration, **(b)** particle size and NaOH concentration, and **(c)** particle size and SMCA loading.

When the NaOH concentration increased, the DS increased from 0.26 (B1) to 0.69 (B8). Furthermore, the DS yields higher at a temperature of 55 °C compared to 35 °C. The same result can be seen when the cellulose: SMCA loading ratio is 1:1.2 compared to 1:1. However, the increase of DS is not linear, indicating an optimum condition is needed. The centre point reflecting the balance between effective substitution and experiments (B9 and B10) shows DS values of (0.56–0.60), confirming good experimental reproducibility and model reliability. The DS values obtained as shown in **Table 5**, ranging from 0.32 to 0.69 are consistent with previous reported findings, where DS values of approximately 0.30 were achieved under mild reaction conditions (Suriyatem et al., 2020). Meanwhile, higher DS values approximately 0.70 have been reported under more intensive parameter conditions (Churam et al., 2024). The slight difference in the responses for B9 and B10 is caused by local conditions in the batch for instance, non-uniform chemical accessibility of cellulose, micro-scale heterogeneity within the same batch of ozonated cellulose, mixing efficiency, heat distribution while mixing and also slight chain degradation in the production process (Fouad et al., 2024; Rahman et al., 2021).

The accuracy and reliability of the model can be confirmed by the parity plot in **Figure 3**, where most of the R^2 values are above 0.8. The model predicting the DS, viscosity and yield (**Figure 3 (a), 3 (b) and 3 (c)**) demonstrates a good reliability between experimental and predicted values, R^2 of 0.99, 0.93 and 0.88. Even though the purity models, **Figure 3 (d)** exhibited a low R^2 value of 0.55. This does not compromise the overall model reliability as the optimization focuses on the DS of CMC.

The significance of each parameter for DS is displayed in **Figure 4**. Based on the standardized effect estimate at a 95% confidence level (α=0.05). All of the parameters have an effect on the DS with the reaction temperature being the strongest individual effect. In addition, several interactions are shown to influence the DS. Specifically, the interaction between NaOH concentration and reaction time (X_1byX_4), reaction temperature (X_1byX_3) and cellulose: SMCA ratio (X_1byX_2) displayed the impact of NaOH concentration on DS depending on other parameters.

The interaction between the parameters and DS were analyzed using a 3D plot as illustrated in **Figure 5**. **Figure 5(a)** shows the red region where the DS is 0.6. The interaction between the NaOH concentration and temperature shows that when the temperature is lower at 34 °C. The NaOH concentration range to achieve DS of 0.6 were quite small at 13-19%. As the temperature increased to 56 °C the NaOH concentration range increased to 10-20%. This outlines that increasing reaction temperatures improves cellulose activation, allowing efficient substitution throughout a broader range of NaOH concentration (Susi et al., 2024).

Figure 5(b) shows the interaction between reaction temperature and reaction time to obtain a DS of 0.6. At a lower reaction time, 1.4-1.5 hrs. The reaction temperature needs to increase to 56 °C. When the reaction time is increased to 2.2 hrs, the reaction temperature range is 48-56 °C. This indicates that extending reaction time allows carboxymethylation reactions to proceed completely even at lower temperatures (Kono et al., 2025).

Table 5 The parameters of the CMC process optimization and its responses

Run	NaOH Conc. (%)	SMCA Loading Ratio	Temp. (°C)	Time (h)	Yield (%)	DS	Purity (%)	Viscosity (cP)
B1	10	1:1	35	1	129.4	0.26	49.5	55.25
B2	20	1:1	35	2	159.9	0.51	67.0	47.74
B3	10	1:1.2	35	2	127.1	0.32	76.5	72.66
B4	20	1:1.2	35	1	130.6	0.32	76.5	87.48
B5	10	1:1	55	2	147.5	0.46	77.0	62.15
B6	20	1:1	55	1	157.7	0.52	65.5	84.02
B7	10	1:1.2	55	1	158.6	0.43	71.0	113.95
B8	20	1:1.2	55	2	206.2	0.69	57.0	84.02
B9 (C)	15	1:1.1	45	1.5	202.8	0.56	65.0	158.84
B10 (C)	15	1:1.1	45	1.5	208.7	0.60	55.5	123.16

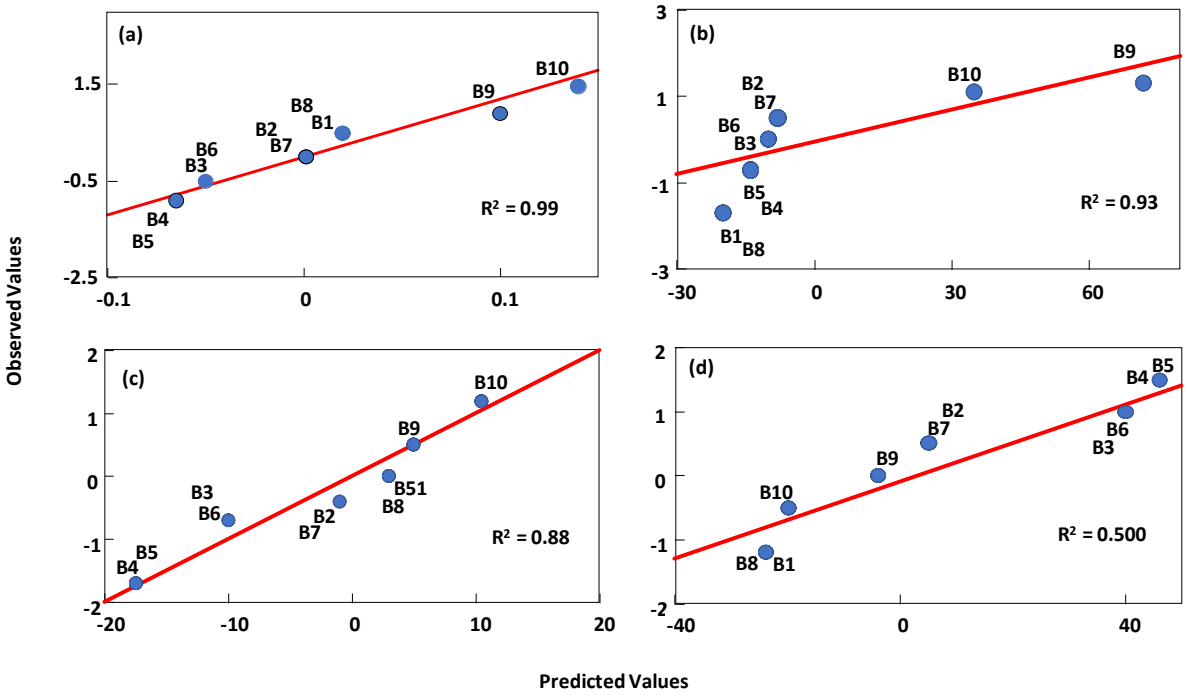

Figure 3 Parity plot for optimization of CMC for **(a)** DS, **(b)** viscosity, **(c)** yield and **(d)** purity

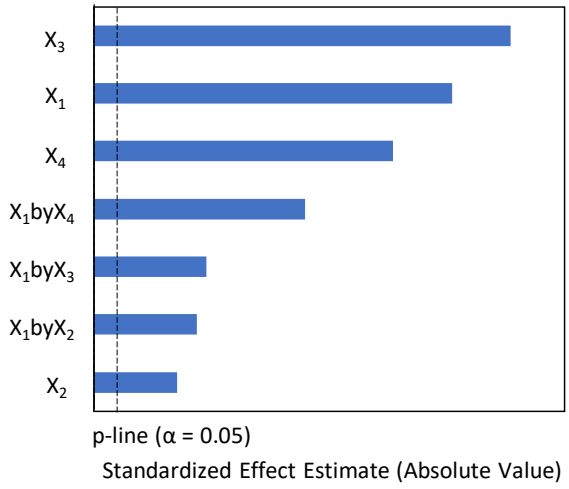

Figure 4 Pareto chart for optimization of CMC parameters for DS (0.6-0.8)

For the interaction between the reaction time and NaOH concentration and its effect on the DS. As visualized in **Figure 5(c)**, higher DS values were obtained at longer reaction times (around 2.2 hrs) and NaOH concentrations between 12% and 22%. As the reaction time decreased to approximately 0.8 hrs, the optimal NaOH range narrowed to about 15-16%. This indicates sufficient alkali swelling is promoted when a longer reaction time is applied, allowing an effective carboxymethylation over a broader range of NaOH concentration (Bogner et al., 2024). Whereas, shorter reaction time restricts the efficiency of the substitution process resulting in narrowing the NaOH concentration range to achieve DS 0.6 (Kono et al., 2025).

Characterization of CMC

To evaluate the thermal stability of CMC with different DS, thermogravimetric (TG) and derivative thermogravimetric (DTG) analyses were performed as depicted in **Figure 6**. Based on the TG curve, all samples exhibited a two-stage degradation pattern. The first stage (30 ℃ to 110 ℃) is the removal of water and the second stage (210 ℃ to 300 ℃) is the degradation of functional groups in the CMC. CMC with DS 0.69 demonstrates a higher percentage of residual weight up to a temperature of 500 °C compared to DS 0.5 and 0.3, indicating a good thermal stability for DS 0.7 among others. In contrast, the sample with DS 0.3 has more weight loss and exhibits the lowest residual mass, showing that DS 0.3 has less resistance to thermal degradation.

The DTG curves display two major degradation peaks for each sample corresponding to distinct thermal decomposition mechanisms. The first peak appears at lower temperature, linked to the removal of water and the initial degradation of the functional groups. The sample with DS 0.69 has the lowest peak compared to DS 0.3. This indicates that higher DS reduces the presence of loosely bound water and thus improves the resistance to the early thermal degradation stage (Celikci et al., 2021). The second peak represents the thermal decomposition of the main cellulose backbone. The same pattern can be seen for DS 0.69, where the second peak is the lowest compared with DS 0.3. Indicating the lower total weight loss in TG Analysis. Overall, CMC with DS 0.69 has high resistance to heat and lower thermal degradation suitable for biofilm fabrication.

The SEM images in **Figure 7** show morphological changes with increasing DS with a magnification of x1000. At DS 0.3, the surface appears compact and smooth, whereas at DS 0.5, the structure becomes slightly rougher with visible surface irregularities. At higher DS (0.69), a more expanded and disrupted structure is observed, indicating increased cellulose modification due to disruption during carboxymethylation.

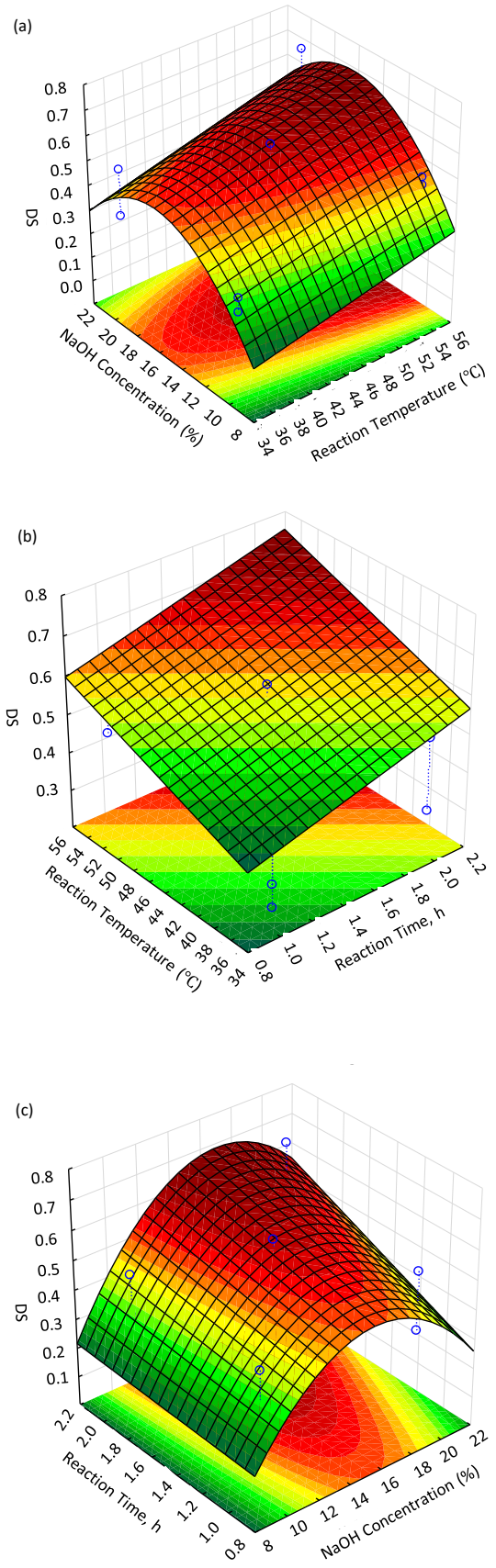

Figure 5 3D Surface plot and contour plot for optimization of parameters for CMC for DS (0.6-0.8): **(a)** NaOH concentration and reaction temperature, **(b)** reaction temperature and reaction time, and **(c)** reaction time and NaOH concentration.

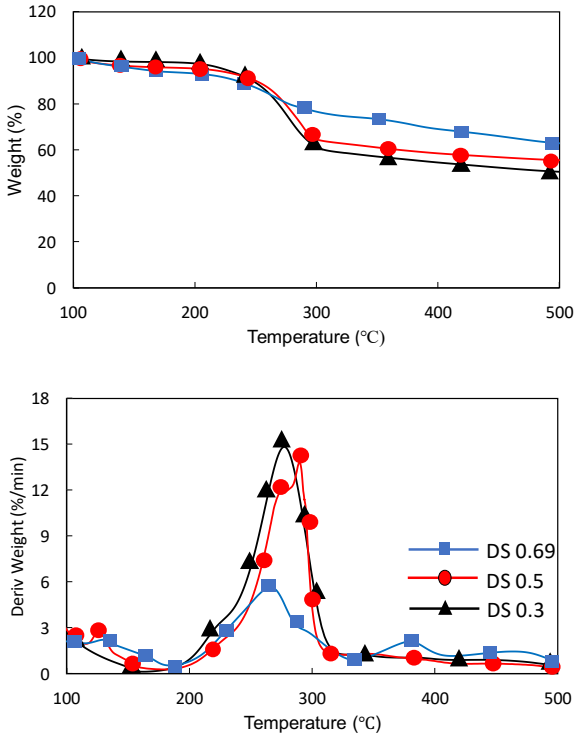

Figure 6 TG-DTG curves for CMC with different DS values

Biofilm Fabrication

Table 6 summarizes the biofilm formulations, mechanical and solubility properties with all the parameters for biofilm. Overall, the results depict that variation of parameters composition strongly influences tensile strength, elongation at break, and water solubility, reflecting the balance between plasticiser, cross-linker, and polymer network formation.

The significance of parameters for each response is illustrated in **Figure 8**, based on the standardized effect estimate at a 95% confidence level (α=0.05). The pareto chart in **Figure 8** demonstrates the significant parameters influencing (a) tensile strength, (b) elongation break, (c) solubility at room temperature and (d) solubility at high temperature. All formulation parameters show a significant effect with CMC and citric acid as a dominant effect. This observation is consistent with the literature, where CMC functions as the primary polymer matrix, providing the fundamental structural framework of the film, while citric acid contributes to enhanced tensile strength through crosslinking interactions that strengthen intermolecular bonding and network integrity (Mahmud et al., 2026). The presence of citric acid promotes the formation of ester linkages, which restrict polymer chain slippage and result in improved mechanical resistance. In contrast, elongation at break is predominantly influenced by the incorporation of plasticizers such as glycerol, which increase chain mobility by reducing intermolecular forces and enhancing flexibility within the polymer network (Sun et al., 2022). This balance between crosslinking density and plasticization is critical, as it governs the trade-off between strength and flexibility, ultimately determining the overall mechanical performance of the biopolymer film.

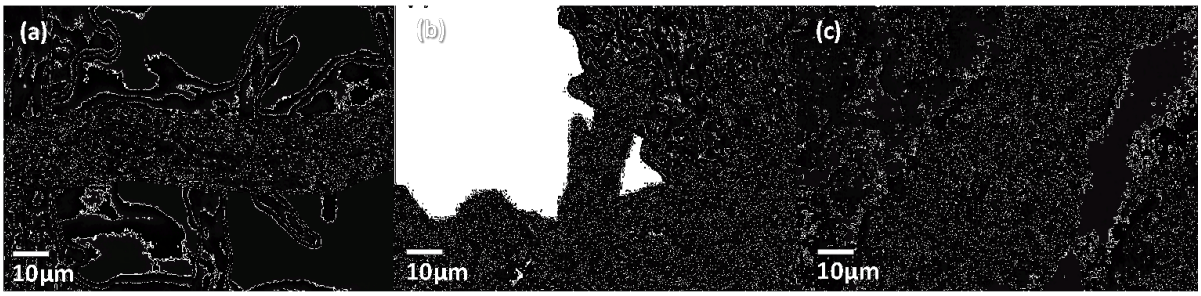

Figure 7 SEM Images of CMC at different DS, (a) CMC with DS 0.3, (b) CMC with DS 0.5 and (c) CMC with DS 0.69

Table 6 Optimal formulation of bioplastic sample alongside its parameters

No.	Glycerol (mL), G_x	Citric acid (g), CA_x	CMC (g),CMC_x	Distilled Water (mL)	Solubility in Water at Room Temp. (%)	Solubility in Water at 100 °C (%)	Tensile Strength (MPa)	Elongation at Break (%)
C1	0.10	1.00	1.50	97.40	6.06	2.41	13.54	12.13
C2	1.00	1.00	1.50	96.50	2.67	0.26	7.88	45.00
C3	0.10	2.50	1.50	95.90	4.64	8.40	1.15	29.00
C4	1.00	2.50	1.50	95.00	4.17	1.89	2.37	21.00
C5	0.10	1.00	5.00	93.90	10.60	73.00	1.08	17.48
C6	1.00	1.00	5.00	93.00	2.32	140.00	0.80	72.67
C7	0.10	2.50	5.00	92.40	3.07	0.08	1.55	79.00
C8	1.00	2.50	5.00	91.50	3.90	0.08	34.43	45.00
C9	0.10	1.00	3.25	95.65	10.50	1.92	2.29	58.50
C10	0.10	2.50	3.25	94.15	1.38	0.33	15.34	36.25
C11	0.10	1.75	1.50	96.65	5.38	0.35	9.30	8.90
C12	0.10	1.75	5.00	93.15	2.74	0.14	1.30	50.00
C13	1.00	1.00	3.25	94.75	4.83	7.93	1.24	73.00
C14	1.00	2.50	3.25	93.25	1.20	4.73	0.77	37.00
C15	1.00	1.75	1.50	95.75	1.04	0.43	0.11	3.00
C16	1.00	1.75	5.00	92.25	4.81	54.00	1.47	78.25
C17	0.55	1.00	1.50	96.95	7.62	6.25	2.83	22.00
C18	0.55	1.00	5.00	93.45	7.56	0.43	0.93	63.50
C19	0.55	2.50	1.50	95.45	18.50	6.60	0.96	15.00
C20	0.55	2.50	5.00	91.95	1.27	0.31	1.06	75.67
C21	0.10	1.75	3.25	94.90	0.03	2.79	1.73	50.00
C22	1.00	1.75	3.25	94.00	73.55	2.67	11.10	76.00
C23	0.55	1.00	3.25	95.20	4.50	2.18	1.86	79.00
C24	0.55	2.50	3.25	93.70	2.32	3.94	0.19	14.00
C25	0.55	1.75	1.50	96.20	5.77	0.16	0.58	27.00
C26	0.55	1.75	5.00	92.70	0.05	0.09	1.50	43.67

However, in this study, CMC and citric acid are the dominant factors according to **Figure 8**. Showing that structural characteristics of the polymer matrix and crosslinking interactions play a more vital role than plasticizers. The effects of CMC are due to its role in forming the polymer network while the citric acid affects the chain mobility via crosslinking. This can enhance the tensile strength and restrict elongation depending on the network structure (Mahmud et al., 2026). Even though the glycerol contributes to the flexibility of biofilm as a plasticizer, its effect is less dominant, which differs from the literature (Sun et al., 2022). This suggests that the mechanical behavior in this biofilm is governed more by network structure and crosslinking rather than plasticization.

To further visualize the interaction effects of each parameter, **Figure 9** depicts the interaction between the parameter and region to achieve high tensile, elongation and low solubility. Based on the contour plot, the region where tensile strength is achieved is 64 MPa at a composition of approximately CMC (0.45-0.64), glycerol (0.3-0.55) and citric acid (0.1–0.3). The highest tensile strength region (>10 MPa) is at moderate CMC content (0.5-0.6), low citric acid (<0.25) and moderate glycerol (0.4-0.5). This shows that a sufficient amount of CMC is needed to form a strong polymer matrix, while excessive citric acid can reduce tensile strength due to over-crosslinking and brittleness (Santos et al., 2026). For the elongation break, the high elongation at 64% can be seen at a region CMC (0.4-0.6), glycerol (0.55-0.8) and citric acid (0.1-0.3). This depicts that glycerol acts as the plasticizer, enhancing the polymer chain mobility and flexibility of the film, with low crosslinker content preventing restriction of chain movement (Hasanin et al., 2025; Kaewprachu et al., 2022).

For solubility at room temperature, low solubility is less than 24% when CMC (0.55-0.8), citric acid (0.35-0.65) and glycerol (0.2-0.45). At high temperature, the solubility is less than 24% when CMC (0.6-0.85), citric acid (0.55-0.75) and glycerol (0.3-0.35). This indicates that while glycerol

promotes solubility and should be kept at low content, increasing CMC will enhance the polymer matrix integrity especially at high temperature, with a moderate amount of citric acid that acts as a crosslinker, strengthening the polymer matrix, allowing the film to resist water penetration better (Rincon et al., 2023; Roy et al., 2021).

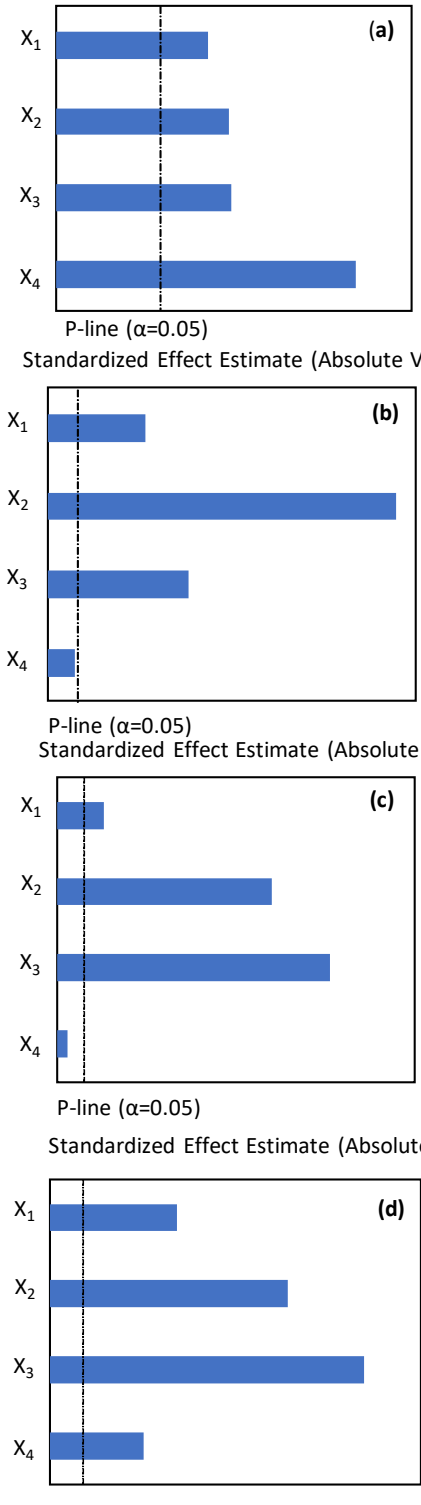

Figure 8 Pareto chart for bioplastic responses (a) tensile strength, (b) elongation break, (c) solubility at room temperature, and (d) high temperature

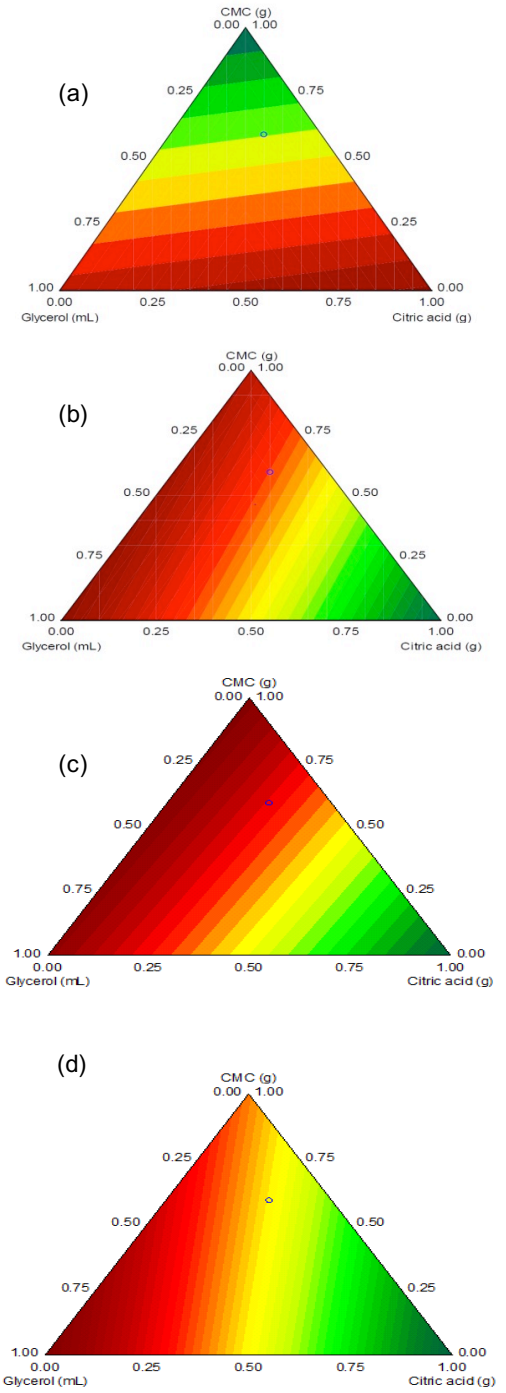

Figure 9 The contour plot for (a) tensile strength, (b) elongation at break, (c) solubility at room temperature and (d) solubility at high temperature.

The comparison between DS values from this study and other studies is presented in **Table 7**. The table indicates ozonated EFB is suitable as a raw material for CMC production. Despite using a moderate NaOH concentration, the DS values obtained remain competitive. **Table 8** demonstrates the properties of biofilm. The tensile strength and solubility of biofilm from this work are within the range reported by (Hidayati et al., 2021; Nazry, 2023), although lower than the value reported by (Hasanin et al., 2025). However, the elongation at break (3–78.25%) from this work is higher than those of the previous studies, indicating improved flexibility due to plasticization and crosslinking,

which results in a balanced performance between tensile and solubility.

Table 7 Comparison of DS values of CMC with literature

Raw Material	NaOH Conc. (%)	SMCA Loading Ratio	DS	Study
Wood pulp cellulose	15 – 30	1:1.2 – 1:1.8	0.2 – 0.8	Rahman et al., 2021
Sugarcane bagasse cellulose	10 – 30	1:1 – 1:2	0.3 – 0.5	Kono et al., 2025
Oil palm	15 – 25	1:1.2	0.6 0.8	Susi et al., 2024
Ozonated EFB	10 – 20	1:1 – 1:2	0.32 – 0.69	This study

Table 8 Comparison of mechanical properties of CMC-based biofilms with literature

Biofilm	σ_s (MPa)	ε_m (%)	Solubility (%)	Study
CMC-based biofilm	23 – 39	20 – 30	30 – 60	Hidayati et al., 2021
CMC-bioplastic	0.25 – 41	4.75 – 19	20 – 50	Nazry et al., 2023
CMC/PVA composite film	70	100	19	Hasanin et al., 2025
CMC-based Biofilm	13 – 34.43	3 – 78.25	24	This study

σ_s, tensile strength; ε_m, elongation at break

As this study focuses on optimization and model development, experimental validation of the predicted optimum conditions was not performed. However, the model's reliability is supported by satisfactory ANOVA, R^2, and lack-of-fit.

CONCLUSION

This study demonstrates effective usage of ozonated EFB-derived CMC for biofilm fabrication. Screening stage identified suitable ranges for DS (0.6–0.8), cellulose-to-SMCA ratio (1:1.6–1:2.2), and NaOH concentration (28–52%). Optimised CMC production with desired DS was achieved at 15% NaOH, 1:2 cellulose-to-SMCA ratio, 55 °C and 1.5 hrs. In biofilm fabrications, moderate CMC (0.5–0.6) and glycerol with low citric acid provided high tensile strength (~64 MPa), while higher glycerol improved flexibility. Moreover, water solubility is reduced with higher CMC content. These findings confirm that enhanced quality biofilms from ozonated EFB-derived CMC can be fabricated with proper formulation.

Acknowledgement

This work is financially supported by Universiti Teknologi Malaysia (UTM), under the Fundamental Research (UTM FR) grant [Q.J130000.3846.22H57].

Conflicts of Interest

The author declares that there is no conflict of interest regarding the publication of this paper.

References

Ab Rasid, N. S., Mohammad Zainol, M., & Saidina Amin, N. A. (2021). Synthesis and characterization of carboxymethyl cellulose derived from empty fruit bunch. *Sains Malaysiana*, *50*(9), 2523-2535. https://doi.org/10.17576/jsm-2021-5009-03

Aisyah, H. A., Hishamuddin, E., Noorshamsiana, A. W., Ibrahim, Z., & Ilyas, R. A. (2024). Oil palm fiber hybrid composites: A recent review. *Journal of Renewable Materials*, *12*(10), 1661-1689. https://doi.org/10.32604/jrm.2024.055217

Bogner, P., Bechtold, T., Pham, T., & Manian, A. P. (2024). Alkali induced changes in spatial distribution of functional groups in carboxymethylated cellulose. *Cellulose*, *31*(5), 2833-2847. https://doi.org/10.1007/s10570-024-05798-9

Çelikçi, N. U. R. A. N., Ziba, C. A., & Dolaz, M. U. S. T. A. F. A. (2022). Synthesis and characterization of carboxymethyl cellulose (CMC) from different waste sources containing cellulose and investigation of its use in the construction industry. *Cellulose Chemistry and Technology, 56*, 55-68.

Churam, T., Usubharatana, P., & Phungrassami, H. (2024). Sustainable production of carboxymethyl cellulose: A biopolymer alternative from sugarcane (*Saccharum officinarum* L.) leaves. *Sustainability*, *16*(6). https://doi.org/10.3390/su16062352

Fouad, H., Jawaid, M., Karim, Z., Meraj, A., Abu-Jdayil, B., Nasef, M. M., & Sarmin, S. N. (2024). Preparation and characterization of carboxymethyl microcrystalline cellulose from pineapple leaf fibre. *Scientific Reports*, *14*(1), 23286. https://doi.org/10.1038/s41598-024-73860-4

Hasanin, M. S., Ibrahim, N. A., & Kamel, S. (2025). Fabrication and characterization of sustainable multifunctional films based on carboxymethyl cellulose and poly (vinyl alcohol) doped with TiO_2 nanoparticles and silicone microemulsion. *Journal of Inorganic and Organometallic Polymers and Materials*. https://doi.org/10.1007/s10904-025-04061-3

Hidayati, S., Zulferiyenni, Maulidia, U., Satyajaya, W., & Hadi, S. (2021). Effect of glycerol concentration and carboxy methyl cellulose on biodegradable film characteristics of seaweed waste. *Heliyon*, *7*(8), e07799. https://doi.org/10.1016/j.heliyon.2021.e07799

Husna, H. Z., Aishah, S. A. N., Nadyaini, W. O. W. N., Sufri, A. M. M., Mba, M. R. M., Thevi, A. P., & Shamjuddin, A. (2025). Parametric studies on delignification using ozonolysis pretreatment of oil palm empty fruit bunch for cellulose nano-fiber production. *Journal of Advanced Research in Micro and Nano Engineering*. https://doi.org/https://doi.org/10.37934/armne.42.1.177204

Kaewprachu, P., Jaisan, C., Klunklin, W., Phongthai, S., Rawdkuen, S., & Tongdeesoontorn, W. (2022).

Mechanical and physicochemical properties of composite biopolymer films based on carboxymethyl cellulose from young palmyra palm fruit husk and rice flour. *Polymers (Basel)*, *14*(9). https://doi.org/10.3390/polym14091872

Kaniapan, S., Hassan, S., Ya, H., Patma Nesan, K., & Azeem, M. (2021). The utilisation of palm oil and oil palm residues and the related challenges as a sustainable alternative in biofuel, bioenergy, and transportation sector: A review. *Sustainability*, *13*(6). https://doi.org/10.3390/su13063110

Kono, H., Kinjyo, S., Uyama, R., Fujita, S., Murayama, Y., & Ikematsu, S. (2025). Biocompatibility and Drug release properties of carboxymethyl cellulose hydrogel for carboplatin delivery. *Gels*, *12*(1). https://doi.org/10.3390/gels12010005

Macieja, S., Sroda, B., Zielinska, B., Roy, S., Bartkowiak, A., & Lopusiewicz, L. (2022). Bioactive carboxymethyl cellulose (CMC)-based films modified with melanin and silver nanoparticles (AgNPs)-The effect of the degree of CMC substitution on the in situ synthesis of AgNPs and Films' Functional Properties. *International Journal of Molecular Sciences,* *23*(24). https://doi.org/10.3390/ijms232415560

Mahmud, J., Heredia, J., Sharaby, M. R., Jaiswal, L., Salmieri, S., Moosavi, S. E., & Lacroix, M. (2026). Development of bioactive carboxymethyl cellulose-based films via dual crosslinking with citric acid and X-ray irradiation. *Foods*, *15*(4). https://doi.org/10.3390/foods15040713

Mahmud, M. S., & Chong, K. P. (2021). Formulation of biofertilizers from oil palm empty fruit bunches and plant growth-promoting microbes: A comprehensive and novel approach towards plant health. *Journal of King Saud University - Science*, *33*(8). https://doi.org/10.1016/j.jksus.2021.101647

Masrullita, Rizka Nurlaila, Zulmiardi, Ferri Safriwardy, Auliani, & Meriatna. (2022). Synthesis carboxyl cellulose (CMC) from rice straw (Oryza sativa L.) waste. *International Journal of Engineering, Science & Information Technology (IJESTY)*, *2*. https://doi.org/10.52088/ijesty.v1i1.200

Nazry, K. N. A. B. K. (2023). *Effect of glycerol and citric acid deep eutectic solvent on the properties of carboxymethyl cellulose bioplastics.* Bachelor Degree Thesis, Universiti Teknologi MARA. https://ir.uitm.edu.my/id/eprint/93624/1/93624.pdf

Nguyen, T. D. P., Le, N. T., Vu, T. M., Pham, T. S., Phan, T. D., Pham, N. L., & Phan, T. T. M. (2022). Synthesis and characterization of carboxymethyl cellulose with high degree substitution from Vietnamese pineapple leaf waste. *Ministry of Science and Technology, Vietnam*, *64*(3), 13-18. https://doi.org/10.31276/vjste.64(3).13-18

Rachtanapun, P., Klunklin, W., Jantrawut, P., Leksawasdi, N., Jantanasakulwong, K., Phimolsiripol, Y., Seesuriyachan, P., Chaiyaso, T., Ruksiriwanich, W., Phongthai, S., Sommano, S. R., Punyodom, W., Reungsang, A., & Ngo, T. M. P. (2021). Effect of monochloroacetic acid on properties of carboxymethyl bacterial cellulose powder and film from nata de coco. *Polymers (Basel)*, *13*(4). https://doi.org/10.3390/polym13040488

Rahman, M. S., Hasan, M. S., Nitai, A. S., Nam, S., Karmakar, A. K., Ahsan, M. S., Shiddiky, M. J. A., & Ahmed, M. B. (2021). Recent developments of carboxymethyl cellulose. *Polymers (Basel)*, *13*(8). https://doi.org/10.3390/polym13081345

Rincon, E., De Haro-Niza, J., Morcillo-Martin, R., Espinosa, E., & Rodriguez, A. (2023). Boosting functional properties of active-CMC films reinforced with agricultural residues-derived cellulose nanofibres. *RSC Advances*, *13*(35), 24755-24766. https://doi.org/10.1039/d3ra04003h

Roy, S., Kim, H.-J., & Rhim, J.-W. (2021). Synthesis of carboxymethyl cellulose and agar-based multifunctional films reinforced with cellulose nanocrystals and shikonin. *ACS Applied Polymer Materials*, *3*(2), 1060-1069. https://doi.org/10.1021/acsapm.0c01307

Santos, M. B., Souza, J. A. d. S., Cândido, V. S., Del Nero, J., Paschoal Junior, W., Maia, A. A. B., Viegas, B. M., Alves Junior, S., Alberto Brito da Silva, C., & Vinícius da Silva Paula, M. (2026). Corn starch/carboxymethyl cellulose films: influence of citric acid on water susceptibility, morphological and tensile properties. *ACS Omega*, *11*(4), 5479-5488. https://doi.org/10.1021/acsomega.5c08949

Song, C.-L., & Othman, J. B. (2022). Synthesis and characterization of lignin-incorporated carboxymethyl cellulose (CMC) films from oil palm lignocellulosic waste. *Processes*, *10*(11). https://doi.org/10.3390/pr10112205

Sun, Z., Tang, Z., Li, X., Li, X., Morrell, J. J., Beaugrand, J., Yao, Y., & Zheng, Q. (2022). The improved properties of carboxymethyl bacterial cellulose films with thickening and plasticizing. *Polymers (Basel)*, *14*(16). https://doi.org/10.3390/polym14163286

Suriyatem, R., Noikang, N., Kankam, T., Jantanasakulwong, K., Leksawasdi, N., Phimolsiripol, Y., Insomphun, C., Seesuriyachan, P., Chaiyaso, T., Jantrawut, P., Sommano, S. R., Ngo, T. M. P., & Rachtanapun, P. (2020). Physical properties of carboxymethyl cellulose from palm bunch and bagasse agricultural wastes: effect of delignification with hydrogen peroxide. *Polymers (Basel)*, *12*(7). https://doi.org/10.3390/polym12071505

Susi, S., Ainuri, M., Wagiman, W., Fajar Falah, M. A., & P, S. K. (2024). Enhanced carboxymethyl cellulose based on empty fruit bunches in a high degree of substitution and thermal stability as a biocomposite film backbone. *International Journal of Chemical Engineering*, *2024*(1). https://doi.org/10.1155/2024/3319401

Thepwat, P., Saenchoopa, A., Onnet, W., Namcharee, P., Sanmanee, C., Plaeyao, K., Kulchat, S., & Kosolwattana, S. (2025). The synthesis and study of carboxymethyl cellulose from water hyacinth biomass stabilized silver nanoparticles for a colorimetric detection sensor of Hg(II) ions. *RSC Advances*, *15*(49), 41241-41252. https://doi.org/10.1039/d5ra04757a

Wahyuni, H. S., Yuliasmi, S., Aisyah, H. S., & Riati, D. (2019). Characterization of synthesized sodium carboxymethyl cellulose with variation of solvent

mixture and alkali concentration. *Open Access Macedonian Journal of Medical Sciences, 7*(22), 3878-3881. https://doi.org/10.3889/oamjms.2019.524

Yuliasmi, S., Ginting, N., Wahyuni, H. S., Sigalingging, R. T., & Sibarani, T. (2019). The effect of alkalization on carboxymethil cellulose synthesis from stem and peel cellulose of banana. *Open Access Macedonian Journal of Medical Sciences*, *7*(22), 3874-3877. https://doi.org/10.3889/oamjms.2019.523

Zhang, H., Su, S., Liu, S., Qiao, C., Wang, E., Chen, H., Zhang, C., Yang, X., & Li, T. (2023). Effects of chitosan and cellulose derivatives on sodium carboxymethyl cellulose-based films: A study of rheological properties of film-forming solutions. *Molecules*, *28*(13). https://doi.org/10.3390/molecules28135211